npg

ORIGINAL ARTICLE

Perpendicular orientation control in thin films of POSS-containing block copolymer domains with a top-coat surface treatment

Takehiro Seshimo[1,2], Yoshiyuki Utsumi[1], Takahiro Dazai[1], Takaya Maehashi[1], Tasuku Matsumiya[1], Yoshinori Suzuki[2], Chiharu Hirano[2], Rina Maeda[2], Katsumi Ohmori[1] and Teruaki Hayakawa[2]

The directed self-assembly of block copolymers (BCPs) can extend the resolution of traditional optical lithographic techniques. Recently, Si-containing BCPs have been shown to produce very small features because they have high χ values. Unfortunately, they cannot be aligned perpendicularly to substrates by thermal annealing because Si-containing blocks exhibit lower surface free energies (SFEs) and tend to form top-wetting layers that are parallel to the substrates. The key factor in achieving orientation control of such types of Si-containing BCPs is SFE control. Three types of newly designed polymers for bottom surface layers (BSLs) that exhibit different SFEs were tested with cylinders forming PMMA-*block*-polyhedral oligomeric silsesquioxane (POSS)-containing poly(methacrylate) (PMMA-*b*-PMAPOSS) and top-coat (TC) materials to prevent the formation of Si-wetting layers. After annealing at 180 °C for 60 min on a hot plate and ashing with oxygen, the samples annealed with TC, and the optimum BSL showed hexagonally packed cylinders; however, the other BSLs did not have perpendicular orientations. To understand these results, the dispersive and polar components of the BSLs, PMMA homopolymer and PMAPOSS homopolymer were compared. The results demonstrated that the relationships between each of the BSL components and homopolymers were found to be more important indicators than the water contact angles.

INTRODUCTION

With the expansion of the use of information technologies in society, semiconductor devices are continually being improved with the aim of lowering their cost, enhancing their performance and increasing their capacity. The integrated circuits in these devices are typically produced by a microfabrication process such as lithography, a technology that has shown remarkable progress in that it can be used to create extremely small patterns even on the nanometer scale. The development of a sub-22-nm manufacturing process, also known as a sub-22-nm node, is the next step in lithography technology. There are many candidate technologies being used to achieve this goal, such as extreme ultraviolet lithography,[1] electron beam lithography,[2] nano-imprint lithography[3] and others.[4] Another remarkable technology is directed self-assembly using block copolymers (BCPs).

Recently, many directed self-assembly techniques based on graphoepitaxy or chemical epitaxy techniques to form aligned BCP patterns have been reported.[5–7] These techniques are being planned not only for making semiconductor applications but also for making imprint templates of bit-patterned media for next-generation storage devices;[8] this is because the technology currently used to generate hard-disk drives is facing physical limits, owing to its thermal

instability. Therefore, directed self-assembly techniques are being studied in various fields, especially because of their expected advantages of high resolution, high throughput, good critical dimension uniformity and low cost.

To date, various types of directed self-assembly techniques have been performed using poly(styrene-*block*-methyl methacrylate) (PS-*b*-PMMA). However, the minimum microdomain dimension that can be achieved with PS-*b*-PMMA is approximately 12 nm because the χ value of PS-*b*-PMMA is not high enough for smaller dimensions. Furthermore, the etch selectivity between PS and PMMA is also too low.[9] Therefore, new types of BCPs are required for use in next-generation applications. Potential candidates for these new BCPs are Si-containing BCPs such as PS-*b*-PDMS,[10,11] poly(4-(pentamethyl disiloxymethyl)-*b*-styrene)[12] and poly(trimethylsilylstyr-ene-*b*-D,L-lactide),[13] and polyhedral oligomeric silsesquioxane (POSS) containing BCPs.[14] These BCPs have higher χ values than PS-*b*-PMMA and have much higher etch selectivity because Si-containing blocks generally show high etch resistance to oxygen plasma etching. Moreover, some of these materials can form sub-10-nm features after solvent annealing. Unfortunately, it is difficult to obtain a perpendicular pattern orientation with these

[1]Tokyo Ohka Kogyo Co., Ltd, 1590 Tabata, Samukawa-machi, Kanagawa, Japan and [2]Department of Organic and Polymeric Materials, Tokyo Institute of Technology, Tokyo, Japan
Correspondence: Professor T Hayakawa, Department of Organic and Polymeric Materials, Tokyo Institute of Technology, 2-12-1-S8-36 O-okayama, Meguro-ku, Tokyo 152-8552, Japan.
E-mail: hayakawa.t.ac@m.titech.ac.jp

Si-containing BCPs by thermal annealing, even if bottom surface layers (BSLs) are applied onto the substrates for neutralization because Si-containing blocks have a lower surface free energy (SFE). Therefore, Si-containing blocks tend to be segregated at the upper surface of BCP thin films, where they can associate with air or nitrogen.

Another solution for achieving perpendicular orientation is the application of the top-coat (TC) process.[15] This concept involves the application of TCs to prevent segregation of the Si-containing block by neutralizing the top interface in the same way as a BSL. The classical approach to control the SFE of a bottom surface is to create a cross-linked or covalently bonded insoluble layer derived from a random copolymer produced from the same monomers as the BCPs. It is not possible to use a random copolymer as a TC because the solvent used to prepare the random copolymer solution would dissolve the BCP film. An excellent method to form a TC on a BCP film would be through a spin-coating method using a polar solvent such as water or methanol. Of course, the polarity of a TC that is soluble in a polar solvent would be too high to neutralize the interface. Ideally, the TC should therefore contain a polarity-switchable unit. One promising candidate for a unit of this nature is maleic anhydride, whose ring-closing reaction is caused by heating and ring-opening reaction is induced by basic aqueous solutions. In this case, the TC material would be stripped from the BCP film with a basic aqueous solution after annealing.

In addition, a BSL composed of random copolymers produced from the same monomers as the BCP is not ideal for a Si-containing BCP because such a BSL would include Si-containing monomers with high etch resistance.[16] Consequently, the BSL would also show a high resistance to oxygen plasma etching. Thus, a BSL for a Si-containing BCP should ideally be composed of non-Si-containing monomers. Moreover, the BSL should function as a neutral layer for the BCP.

This paper reports the results of our studies on the materials design of a neutral layer of BSLs for a high-resolution Si-containing BCP of PMMA-*b*-PMAPOSS. To optimize a BSL for perpendicular orientation of PMMA-*b*-PMAPOSS cylinders, we focused on the water contact angles, a dispersive component and a polar component in the SFEs.

EXPERIMENTAL PROCEDURE

Materials

PMMA-*b*-PMAPOSS diblock copolymers were synthesized by living anionic polymerization according to a procedure from a previously published report.[14] The chemical structure and composition of the resulting PMMA-*b*-PMAPOSS were characterized by ^1H and ^{13}C NMR spectra. The unit mole ratio of PMMA/PMAPOSS (78:22) was calculated from the ^{13}C NMR spectrum by using the ratio of the integrated intensities of the signals for the carbonyl carbon and the methylene carbon adjacent to Si. The number-average molecular weight (M_n) and polydispersity index of PMMA-*b*-PMAPOSS against linear PS standards were 15 500 g mol^{-1} and 1.02, respectively. The T_g of PMAPOSS was 82 °C.[17] The volume ratio of PMMA/PMAPOSS was 28:72, as determined on the basis of the ^{13}C NMR spectrum and the individual component densities of 1.15 and 1.13 g cm^{-3}, respectively, which were measured using the density gradient tube method.[18]

EETTB (1-ethenyl-4-[1-(ethoxymethoxy)-2,2,2-trifluoro-1-(trifluoromethyl) ethyl]-benzene; Supplementary Figure S1) was synthesized in the usual manner from 1,1,1,3,3,3-hexafluoro-2-(4-vinylphenyl)propan-2-ol and chloromethyl ethyl ether. Maleic anhydride, norbornene, EETTB and azobisisobutyronitrile were mixed in tetrahydrofuran. The polymerization was performed at 60 °C for 48 h. After purification, the polymer was reacted with 28 wt% ammonium hydroxide (NH$_4$OH). The TC-A was precipitated in ethyl acetate to yield a white powder that was dried *in vacuo*. The chemical structure and composition of the resultant TC-A were characterized by ^1H, ^{13}C and ^{19}F NMR. The NMR results indicated that the ratio of the maleic anhydride, norbornene and EETTB repeating units was 49:27:24.

4-*Tert*-butylstyrene, 3-(trifluoromethyl)styrene or styrene (St) and methacrylic acid were copolymerized with azobisisobutyronitrile. The BSL-A, BSL-B and BSL-C polymers were precipitated in a mixture of methanol and water to yield a white powder that was dried *in vacuo*. The chemical structure and composition of the resulting BSLs were characterized by ^1H and ^{13}C NMR
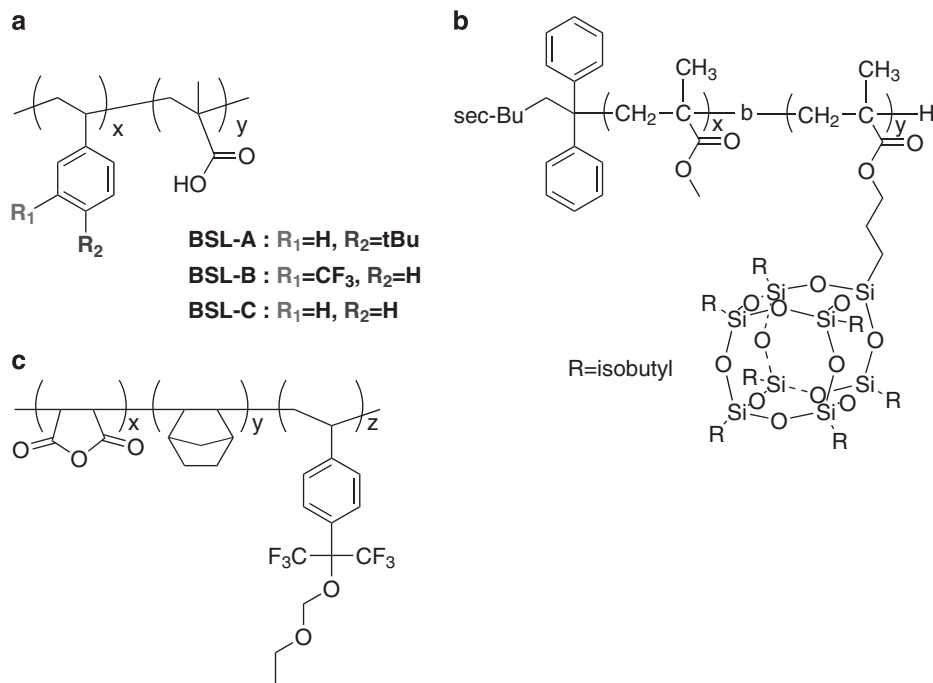

Figure 1 Chemical structures of (**a**) the three BSLs, (**b**) PMMA-*b*-PMAPOSS and (**c**) TC-A. BSL, bottom surface layer; PMMA-*b*-PMAPOSS, poly(methyl methacrylate)-*block*-polyhedral oligomeric silsesquioxane (POSS)-containing poly(methacrylate); TC, top-coat. A full color version of this figure is available at *Polymer Journal* online.

(Supplementary Figure S2–S4), and the M_n and the polydispersity index were measured using gel permeation chromatography. To reveal the differences in the SFEs of the BSLs, the contact angles of the BSL films were measured. For this experiment, the BSLs were dissolved in propylene glycol monomethyl ether acetate (PGMEA). The solution was spin coated onto a Si wafer to form a 10 nm film, and the wafer was baked at 230 °C for 1 min. After cooling, the wafer was treated with PGMEA to remove any residual polymers on the wafer. After the post-baking process carried out at 110 °C for 1 min, the static contact angles were measured with H_2O and diiodomethane (CH_2I_2) with a DM-501 (Kyowa Interface Science, Saitama, Japan). The Wu equation (Equation S1) was applied to obtain the SFE of the dispersive and polar components of the BSL films.[19] The contact angles of the PMMA and PMAPOSS homopolymers were also measured.

The structures of PMMA-b-PMAPOSS, TC-A, BSL-A, BSL-B and BSL-C are shown in Figure 1.

Methods

The BSLs were dissolved in PGMEA and spin coated onto a Si wafer to form films with a thickness of 10 nm. The film thickness was measured with a Nanospec M3000 (Nanometrics, Milpitas, CA, USA). The wafer was then baked at 230 °C for 1 min and washed with PGMEA. PMMA-b-PMAPOSS was dissolved in PGMEA and spin coated onto the BSL film to form films with a thickness of 25 nm; the wafer was then baked at 110 °C for 1 min. TC-A was dissolved in a mixture of water–methanol (1:3 by weight) and spin coated onto the PMMA-b-PMAPOSS film to form a 60 nm film. The wafer was then annealed at 180 °C for 60 min on a hot plate. After being allowed to cool, the wafer was treated with a mixture of 28 wt% NH_4OH–methanol (1:3 by weight) to remove the TC-A film. Oxygen ashing was carried out in a vacuum chamber to remove the PMMA block. The oxygen flow rate was set to 200 ml min^{-1} and the applied voltage was 200 W. The remaining film thickness was measured

to obtain ashing amounts of the homopolymers. Scanning electron microscopy observations were performed with a S-4700 (Hitachi High-Technologies Corporation, Tokyo, Japan).

RESULTS AND DISCUSSION

The polymer characterization data, measured contact angles and calculated SFEs of the BSLs and homopolymers used in this study are summarized in Table 1.

The results of the ashing measurements are shown in Figure 2a. The ashing time was determined to be 1 min based on the pre-ashing examination using PMMA and PMAPOSS homopolymer films. The amount of ashing for PMMA was observed to be approximately five times higher than that for PMAPOSS under these conditions. The flow of the experimental process is shown in Figure 2b.

The scanning electron microscopy images after ashing, together with schematic diagrams showing the layers used for film preparation are shown in Figures 3a–e; observations showed that only the combination of BSL-A and TC-A yielded well-ordered perpendicular cylinders (d spacing of 25 nm; Figure 3a). However, neither BSL-B nor BSL-C in combination with TC-A appeared to yield cylinders parallel to the substrate (Figures 3b and c). When only TC-A or BSL-A was used, no perpendicular cylinders were observed (Figures 3d and e). These results indicated the necessity of combining a BSL and a TC with suitable SFEs to generate perpendicular cylinders.

The water contact angles of BSL-A and BSL-B were almost identical but differed from that of diiodomethane (Table 1), which reflected the different SFEs of the different films. In the case of the BSL that was derived from a random copolymer made from the same monomers as the BCP, the SFE could be optimized by changing the monomer ratio in the BSL. However, one of the monomers needed to be replaced because of etching transfer issues of the Si-containing monomers; in this case, the SFE would become an important indicator for the selection of an appropriate substitution unit for the Si-containing monomer.

The relationship between the BSL and the perpendicular cylinder oriented PMMA-b-PMAPOSS was investigated in the component map of the SFEs. The SFE is defined as the sum of the energy of a dispersive component (d) and a polar component (p). The interfacial energy between homopolymers composed of BCPs and BSLs is expressed in Equation S2.[20] The d and p components of each material were compared by plotting their respective square roots on a component map. Figure 4 shows the component maps of PMMA, PMAPOSS and BSLs. The distance between two points is proportionate to the square root of the interfacial energy in this map. Under the assumption that the contact area of the perpendicularly oriented nanostructures on a

Table 1 Characterization of polymers with contact angles and calculated surface free energies (SFEs)

				Contact angle (°)		SFE[a] (mN m^{-1})		
	Composition	M_n	PDI	H_2O	CH_2I_2	d	p	Total
BSL-A	TBSt/MAA = 95/5	27 900	1.75	102	49	38.5	0.5	39.0
BSL-B	3-TFMSt/MAA = 97/3	36 200	1.70	99	63	25.3	3.8	29.1
BSL-C	St/MAA = 97/3	21 300	1.72	86	32	37.5	6.2	43.7
PMMA	—	9800	1.03	68	39	30.1	16.1	46.2
PMAPOSS	—	7000	1.04	104	48	40.4	0.0	40.4

Abbreviations: BSL, bottom surface layer; MAA, methacrylic acid; PDI, polydispersity index; M_n, number-average molecular weight; PMAPOSS, polyhedral oligomeric silsesquioxane (POSS)-containing poly(methacrylate); PMMA, poly(methyl methacrylate); St, styrene; TBSt, 4-tert-butylstyrene; 3-TFMSt, 3-(trifluoromethyl)styrene.
[a]d: dispersive components of SFE, p: polar component of SFE, total: sum of dispersive and polar components.
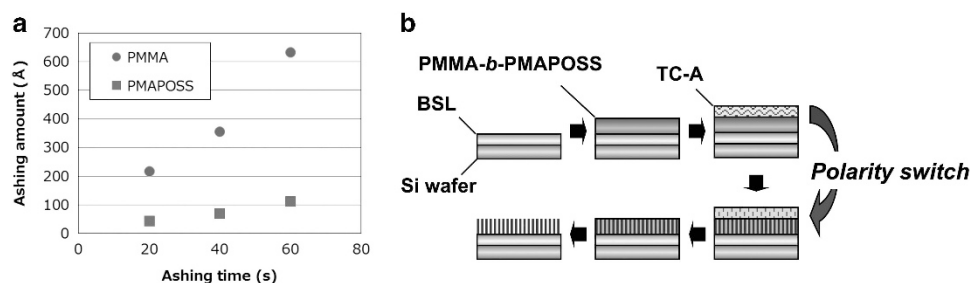

Figure 2 (a) Amounts of ashing for PMAPOSS and PMMA homopolymers. (b) Schematic of the pattern formation process using TC-A. BSL, bottom surface layer; PMMA-b-PMAPOSS, poly(methyl methacrylate)-block-polyhedral oligomeric silsesquioxane (POSS)-containing poly(methacrylate); TC, top-coat. A full color version of this figure is available at Polymer Journal online.
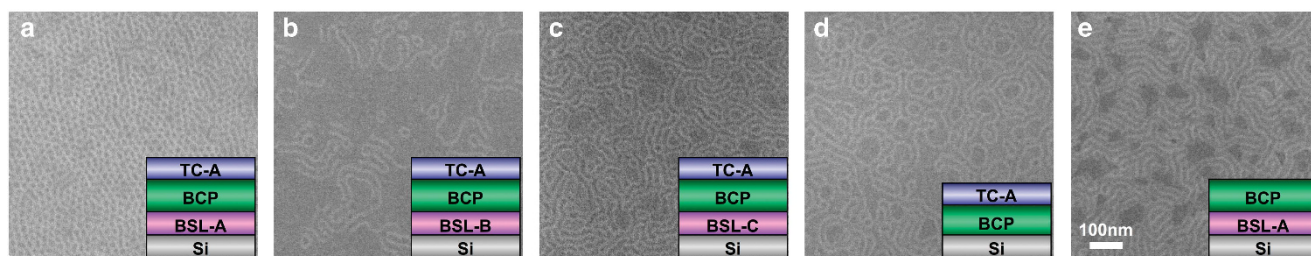
Figure 3 SEM images of structures and schematic illustrations for film preparation formed on (**a**) BSL-A, (**b**) BSL-B, (**c**) BSL-C, (**d**) bare Si with TC-A and (**e**) BSL-A without TC-A. BCP, block copolymer; BSL, bottom surface layer; PMMA-*b*-PMAPOSS, poly(methyl methacrylate)-*block*-polyhedral oligomeric silsesquioxane (POSS)-containing poly(methacrylate); SEM, scanning electron microscopy; TC, top-coat.
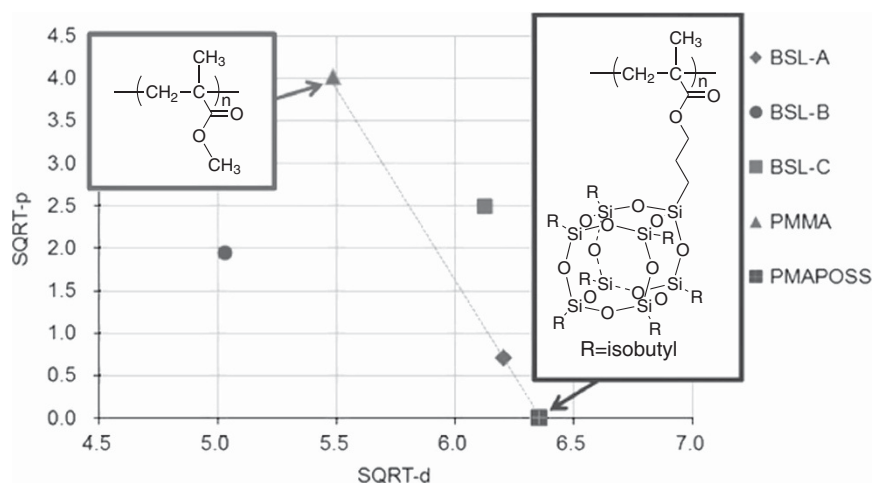

Figure 4 Component map from measured SFEs. BSL, bottom surface layer; PMMA, poly(methyl methacrylate); PMAPOSS, polyhedral oligomeric silsesquioxane (POSS)-containing poly(methacrylate); SFE, surface free energy; SQRT, square root. A full color version of this figure is available at *Polymer Journal* online.

BSL corresponded to the volume ratio of the BCPs, the interfacial energy between the BCP and the BSL could be calculated. These results are shown in Supplementary Figure S5.

The point for BSL-A on the map is suitable for supporting the perpendicular cylinders and falls on the straight line connecting the points for PMMA and PMAPOSS. This point is located in the region of the nearly lowest interfacial energy. However, the points for BSL-B and C, which do not form perpendicular cylinders, are plotted in a region with higher interfacial energy than BSL-A. This is in good agreement with the experimental results. A similar tendency was observed in PS-*b*-PMMA with PS-*random*-PMMA (PS-*r*-PMMA) copolymers.[21] Therefore, this method is very useful for estimating the degree of affinity between the BSLs and BCPs, especially for BSLs composed of different monomers in the BCPs. To achieve a perpendicularly oriented BCP domain, it was essential to use not only BSL but also TC. Unfortunately, this method cannot be applied to the TC because the lower surface of the TC cannot be evaluated by contact angle measurements and is in contact with the upper surface of the BCPs. One method to evaluate the neutralization layer of TC has been previously reported.[22] The combination of these evaluation methods will allow for the further understanding and development of TC processes, which will enable the orientation of high-resolution Si-containing BPCs to be controlled by manufacturing-friendly thermal annealing processes.

CONCLUSIONS

In summary, we demonstrated the orientation control of PMMA-*b*-PMAPOSS with thermal annealing. In particular, three types of BSLs with different surface properties were tested. In addition, a material whose polarity could be changed was used as a TC to prevent the formation of a wetting layer composed of Si-containing units. It was found that the combination of BSL-A and TC-A yielded perpendicular cylinders after annealing at 180 °C for 60 min, whereas the other combinations produced parallel cylinders. These results indicated that it is necessary to control the surface properties of both the bottom and top surfaces of the BCP films. However, the indicators of the surface properties of perpendicularly oriented Si-containing BCPs were not revealed because the BSLs for Si-containing BCPs needed to be replaced with non-Si-containing monomers. In this study, the water contact angles and the SFEs were compared as indicators to evaluate the neutrality of BSL to the perpendicularly orientated PMMA-b-PMAPOSS cylinders. It was revealed that SFEs were more effectual indicators than water contact angles, and the component map clearly indicated the relationship between each component of the SFE and the interfacial energy. The correlation on the map also indicated suitable SFE regions for perpendicular orientation, which depended on the volume ratio of the BCPs. In addition, it was possible to substitute one of the monomers of BSL with non-Si-containing monomers to achieve perpendicularly oriented Si-containing BCP domains, given that the substituted monomer had a suitable SFE.

CONFLICT OF INTEREST

The authors declare no conflict of interest.

1 Stulen, R. H. & Sweeney, D. W. Extreme ultraviolet lithography. *IEEE J. Quantum Electron.* **35**, 694–699 (1999).

2 Pfeiffer, H. C. Direct write electron beam lithography: a historical overview. *Proc. SPIE* **7823**, 7823161–7823166 (2010).

3 Malloy, M. & Litt, L. C. Technology review and assessment of nanoimprint lithography for semiconductor and patterned media manufacturing. *J. Micro Nanolithogr. MEMS MOEMS* **10**, 0320011–03200113 (2011).

4 Yaegashi, H., Oyama, K., Yabe, K., Yamauchi, S., Hara, A. & Natori, S. Novel approaches to implement the self-aligned spacer double-patterning process toward 11-nm node and beyond. *Proc. SPIE* **7972**, 79720B1–79720B7 (2011).

5 Ruiz, R., Kang, H., Detcheverry, F. A., Dobisz, E., Kercher, D. S., Albrecht, T. R., de Pablo, J. J. & Nealey, P. F Density multiplication and improved lithography by directed block copolymer assembly. *Science* **321**, 936–939 (2008).

6 Cheng, J. Y., Mayes, A. M. & Ross, C. A. Nanostructure engineering by templated self-assembly of block copolymers. *Nat. Mater.* **3**, 823–828 (2004).

7 Bita, I., Yang, J. K. W., Jung, Y. S., Ross, C. A., Thomas, E. L. & Berggren, K. K. Graphoepitaxy of self-assembled block copolymers on two-dimensional periodic patterned templates. *Science* **321**, 939–943 (2008).

8 Wan, L., Ruiz, R., Gao, H., Patel, K. C., Lille, J., Zeltzer, G., Dobisz, E. A., Bogdanov, A., Nealey, P. F. & Albrecht, T. R. Fabrication of templates with rectangular bits on circular tracks by combining block copolymer directed self-assembly and nanoimprint lithography. *Proc. SPIE* **8323**, 8323191–83231914 (2011).

9 Farrell, R. A., Petkov, N., Shaw, M. T., Djara, V., Holmes, J. D. & Morris, M. A. Monitoring PMMA elimination by reactive ion etching from a lamellar PS-b-PMMA thin film by *ex situ* TEM methods. *Macromolecules* **43**, 8651–8655 (2010).

10 Huda, M., Akahane, T., Tamura, T., Yin, Y. & Hosaka, S. Fabrication of 10-nm-order block copolymer self-assembled nanodots for high-density magnetic recording. *Jpn. J. Appl. Phys.* **50**, 06GG061–06GG065 (2011).

11 Gotrik, K. W., Hannon, A. F., Son, J. G., Keller, B., Alexander-Katz, A. & Ross, C. A. Morphology control in block copolymer films using mixed solvent vapors. *ACS Nano* **6**, 8052–8059 (2012).

12 Fukukawa, K., Zhu, L., Gopalan, P., Ueda, M. & Yang, S. Synthesis and characterization of silicon-containing block copolymers from nitroxide-mediated living free radical polymerization. *Macromolecules* **38**, 263–270 (2005).

13 Cushen, J. D., Bates, C. M., Rausch, E. L., Dean, L. M., Zhou, S. X., Willson, C. G. & Ellison, C. J. Thin film self-assembly of poly(trimethylsilylstyrene-b-D,L-lactide) with sub-10 nm domains. *Macromolecules* **45**, 8722–8728 (2012).

14 Hirai, T., Leolukman, M., Hayakawa, T., Kakimoto, M. & Gopalan, P. Hierarchical nanostructures of organosilicate nanosheets within self-organized block copolymer films. *Macromolecules* **45**, 4558–4560 (2008).

15 Bates, C. M., Seshimo, T., Maher, M. J., Durand, W. J., Cushen, J. D., Dean, L. M., Blachut, G., Ellison, C. J. & Willson, C. G. Polarity-switching coats enable orientation of sub–10-nm block copolymer domains. *Science* **338**, 775–779 (2012)

16 Hirai, T., Leolukman, M., Liu, C. C., Han, E., Kim, Y. J., Ishida, Y., Hayakawa, T., Kakimoto, M., Nealey., P. F. & Gopalan, P. One-step direct-patterning template utilizing self-assembly of POSS-containing block copolymers. *Adv. Mater.* **21**, 4334–4338 (2009).

17 Goseki, R., Hirai, T., Ishida, Y., Kakimoto, M. & Hayakawa, T. Rapid and reversible morphology control in thin films of poly(ethylene oxide)-block-POSS-containing poly (methacrylate). *Polym. J.* **44**, 658–664 (2012).

18 Tada, Y., Yoshida, H., Ishida, Y., Hirai, T., Bosworth, J. K., Dobisz, E., Ruiz, R., Takenaka, M., Hayakawa, T. & Hasegawa, H. Directed self-assembly of POSS containing block copolymer on lithographically defined chemical template with morphology control by solvent vapor. *Macromolecules* **45**, 292–304 (2012).

19 Wu, S. Calculation of interfacial tension in polymer systems. *J. Polym. Sci. Part C* **34**, 19–30 (1971).

20 Owens, D. K. & Wendt, R. C. Estimation of the surface free energy of polymers. *J. Appl. Polym. Sci.* **13**, 1741–1747 (1969).

21 Han, E., Stuen, K. O., La, Y. H., Nealey, P. F. & Gopalan, P. Effect of composition of substrate-modifying random copolymers on the orientation of symmetric and asymmetric diblock copolymer domains. *Macromolecules* **41**, 9090–9097 (2008).

22 Maher, M. J., Bates, C. M., Blachut, G., Sirard, S., Self, J. L., Carlson, M. C., Dean, L. M., Cushen, J. D., Durand, W. J., Hayes, C. O., Ellison, C. J. & Willson, C. G. Interfacial design for block copolymer thin films. *Chem. Mater.* **26**, 1471–1479 (2014).

Supplementary Information accompanies the paper on Polymer Journal website (http://www.nature.com/pj)